Received: 1 April 2022 | Revised: 8 July 2022 | Accepted: 12 July 2022

DOI: 10.1002/ese3.1355

ORIGINAL ARTICLE

Experimental validation of fuzzy type-2 against type-1 scheme applied in DC/DC converter integrated to a PEM fuel cell system

Cristian Napole | **Mohamed Derbeli** | **Oscar Barambones**

Department of Systems Engineering and Automation Engineering School of Vitoria, Basque Country University (UPV/EHU), Vitoria, Spain

Correspondence
Cristian Napole and Oscar Barambones, Department of Systems Engineering and Automation, Engineering School of Vitoria, Basque Country University (UPV/EHU), Vitoria, Araba 1006, Spain.
Email: cristianmario.napole@ehu.eus and oscar.barambones@ehu.eus

Funding information
Diputación Foral de Álava, Grant/Award Number: CONAVANTER; Euskal Herriko Unibertsitatea, Grant/Award Number: GIU10/063; Eusko Jaurlaritza, Grant/Award Number: ELKARTEK KK-2021/00092

Abstract

This research presents and compares the outcomes of experimental implementations of different fuzzy logic control structures for a proton exchange membrane fuel cell (PEMFC). These devices are well known for their capability to transform chemical energy into electrical with low emissions. Commonly, a PEMFC has a linkage with a boost converter which allows a suitable end-user voltage through a nonlinear control law. Hence, the contribution in this sense is the experimental comparison of two fuzzy logic strategies known as type-1 and type-2 that were implemented in a PEMFC system. The approaches were embedded in a control board dSPACE 1102 which also has the capability to acquire data. The contrast of results showed capabilities improvement against disturbances in terms of error reduction, control signal, and robustness.

KEYWORDS

fuzzy control, fuzzy logic, fuzzy set, PEMFC, renewable energies, sliding mode control

1 | INTRODUCTION

Renewable energies resources (RES) are currently a trending topic in terms of the replacement of fossil sources commonly known for their harmful consequences in the environment.[1] Fuel cells are a suitable RES device due to their efficiency which arises 60%, which is one of the highest values in comparison with photovoltaic panels (between 6% and 20%) or wind turbines (around 25%).[2,3] Currently, proton exchange membrane fuel cells (PEMFC) are an innovative technology in countries like China. Although that is one of the major producers of industrial pollution due to coal consumption which is around half of the global demand, the installed capacity of PEMFC had produced 46MW only in public transport in 2021.[4,5]

Commercial PEMFC output voltages can reach up to 50 V.[6] However, this value is low for industrial applications such as automotive which require more than 10 times extra.[7] Boost converters (also known as "step-up") are known for these purposes where an end-user voltage is required to be higher than the one from the source.[8] Additionally, few elements define a boost converter topology which concludes with advantages such as simple design, low voltage stress, and high efficiency.[9] Moreover, a boost converter linked to devices provides a system efficiency increase by the design of an appropriate control law that can track the required voltage or current.[10]

Linear controllers from classic control theory had been implemented by researchers in converters combined with PEMFC. For instance, linear quadratic regulator (LQR) is a strategy which the objective to find a quadratic performance index through an offline minimization to achieve a suitable control law for a system.[11] An example of a simulated PEMFC system has been performed by authors Kodra and Zhang,[12] where they developed a high-order plant for different time scales and aimed to control the fuel flow with an LQR. They were able to achieve suitable responses in terms of flow control from the simulated hardware. Another linear known linear approach is proportional-integral-derivative (PID), which has been implemented for a PEMFC aiming to control fuel cell flow in Woo et al.[13] Results showed an acceptable regulation of fuel cell reactants although the authors developed the strategies without comparison to similar approaches. In terms of boost converters, a PID was analyzed against advanced controllers such as an internal mode controller (IMC) or sliding mode control (SMC).[14] They showed that a major issue of PID was the tuning gain process because even with suitable parameters, the behavior is unsatisfactory. In the review made, the main issue related to linear controllers applied to real-time systems is the narrow range of operation which limits the prior design and can lead to an instability state which is undesirable.[15] Moreover, linear controllers in boost converters tend to yield an inconsistency related to the intrinsic nonminimum phase.[16]

Boost converters have a nonlinear behavior due to their switching states and perturbations,[2] thus advanced controllers need to be considered. Fractional-order proportional-derivative-integral (FOPID) is a nonlinear extension of the conventional approach with extra orders which induces more flexibility to achieve requirements.[17] Authors in ref[18] designed a cascade control for a DC-DC converter using a FOPID by facing the nonminimum phase issue that boosts converters have. They showed acceptable capabilities for disturbance rejection in a real-time implementation, although the parameter tuning had to be performed offline through an optimization algorithm. Nevertheless, this procedure can generate a difference in the implementation due to scenario variation. Actually, this design has certain disadvantages related to: (1) if the primary process of the cascade control owns a significant delay, it can degrade the system performance[19] and (2) FOPIDs are expensive to produce for industrial purposes due to the fractional approximation.[20] The PID also has been proposed by authors of[21] where they used the fuzzy logic control (FLC) for the parameter tuning process. Obtained results have shown that the proposed method guarantees high performance around the equilibrium point and under parametric uncertainty. Besides, considerable improvement in the response time and control robustness also was achieved. A nonlinear control that can counteract these issues is sliding mode control (SMC) which is known for its robustness against uncertainties and simple implementation.[22] A simulated implementation of SMC has been performed by authors of Abbaker et al.,[23] where they used it for oxygen supply regulated with an estimation algorithm for the unknown dynamics. Results showed sufficient robustness and performance increase as well as a fast convergence. On the other hand, an example of the implementation of SMC in a converter has been shown by Huanfu et al.[24] In this case, they embedded an SMC to achieve the minimum input power by phase angle control and voltage regulation. Experimental results showed improvements in robustness and settling time which were beneficial for device protection. Nevertheless, a main drawback of SMC is chattering which is the cost of the high robustness that is generated by discontinuous control law.[25] Several solutions had appeared during the recent decades and probably the most efficient one is the super-twisting algorithm (STA).[26] This tool is a dynamic extension that generates a continuous control integrated signal that shadows the discontinuity of the SMC.[27] A disadvantage of this structure is the slow convergence and settling time caused by the tuning gains.[28] However, to speed up the convergence, authors of Rakhtala and Casavola[29] have proposed a cascade structure for the STA. A comparison study with the conventional SMC, terminal SMC, and adaptive SMC has shown the effectiveness of the proposed structure in terms of accuracy and convergence speed.

Another well-known nonlinear approach is fuzzy logic control (FLC), which essential feature is design flexibility as it can be tuned by an expert with knowledge of a particular system to be controlled.[30] This can be performed through simple definitions of rules that a human emulates by linguistic rules.[31] Not only it has the capabilities to be used as a controller but also as a system identification when mathematics tends to be complex.[32] In the review made by Yang et al.,[33] they found that FLC is a well-used structure that can provide better performance than conventional controllers and it can be used with satisfactory outcomes in PEMFC systems. Authors Samadi and Rakhtala[34] have proven that FLC can show great performance especially when it is applied to power converters. Fuzzy structures were established by the discoverer Lofti Zadeh, which are known as fuzzy sets type-1 and -2 (in control systems, these are known as FLC-T1 and FLC-T2).[35,36] The latter mentioned has the advantage to handle uncertain definitions in which the

designer has doubts and this ambiguity can be mirrored numerically during the controller's initial configuration. Fuzzy sets type-3 also has been proposed by several researchers.[37–40] For instance, authors of Mosavi et al.[37] have developed a fractional-order control system based on fuzzy type-3. The proposed algorithm has been compared with several control methods such as PID, SMC, LQR, and passivity-based control systems (PBC), where the results have demonstrated significant superiority of the suggested algorithm. Authors of Liu et al.[38] have proposed an interval type-3 fuzzy logic system (IT3-FLSs) combined with an online learning approach. Obtained results have shown the high performance of the schemed method when compared to some other well-known methods.

Therefore, based on the background research made, the main contributions of this article are as follows:

- The implementation of FLC-T1 and FLC-T2 schemes in a commercial PEMFC system linked to a boost converter. Our intention is to track the desired current and seek high performance in accuracy and generated control signal.
- The experimental outcomes with an in-depth comparative analysis of robustness, accuracy, and response time. These are important features to be studied because the improvement of these characteristics is mainly connected to the system efficiency enhancement.

The structure of this article is arranged as follows in accordance with the structure from the figure Table of Contents. Section 2 introduces the commercial hardware involved that has been used in the experiments with its details. Additionally, this was split in Sections 2.2, 2.3, and 2.4 which, respectively, are about (1) the model and performance index for control tuning, (2) design details of FLC-T1, and (3) further facts of the extension to FLC-T2. The experimental outcomes are analyzed in Section 3. Finally, a summary of the work is provided in Section 4.

2 | MATERIALS AND METHODS

2.1 | Employed hardware

In this research, we designed a platform for real-time experiments aiming at the implementation of controllers which could enhance the system's performance. The main device to be studied is a PEMFC from the manufacturer Heliocentris whose model is FC50. This PEMFC is fed with high-purity hydrogen (99.999%) compressed at 1 MPa. The FC50 is capable to generate 5VCC as output voltage with a current between 8 and 10 A and a power above 40 W. The security measures designed by the manufacturer are the inclusion of a safety circuit that controls variables like fuel supply, oxygen, humidity, and stack temperature. Further details are in Table 1.

TABLE 1 Heliocentris PEMFC FC50

	Values
Heliocentris PEMFC FC50	
Operating voltage	2.5–9 VDC
Operating current	0–10 A
Rated output power	40 W
Open-circuit voltage	9VDC
Boost converter TEP192	
Inductance	6 μH
Input capacitor	1500 μF
Output capacitor	3000 μF
Max. input voltage	60 V
Max. input current	30 A
Max. output voltage	250 V
Max. output current	30 A

We linked the PEMFC with a boost converter TEP-192. With the help of a metal-oxide-semiconductor-field-effect-transistor (MOSFET), we controlled the boost converter through a pulse-width-modulation (PWM) signal at a maximum frequency of 20 kHz. We used the modeled circuit from Figure 1. The basic electric elements of the circuit are an inductor (L), a capacitor (C), a diode (D), a switching device (S_1), and an external load (R). The external load hardware is a single output resistance for DC loads known as BK Precision 8500. It is a digital programmable resistance that can be set between 0.1 and 1000 Ω. Also, it can handle a maximum power of 120 W and a voltage of 115 V at a top frequency of 47 Hz.

Acquisition and control of the boost converter were performed with a dSPACE MicroLabBox DS1202 as this has the capacity to generate a PWM signal. This is a flexible and trustworthy device for mechatronics research and development due to its robustness for high-performance testing. The 100 signal channels that it possesses for input/output, are able for digital, analog, or PWM. The inner electronics is based on a dual-core processor with a maximum frequency of 2 GHz that is linked with a programmable FPGA. DSPACE also included the real-time-interface (RTI) platform to

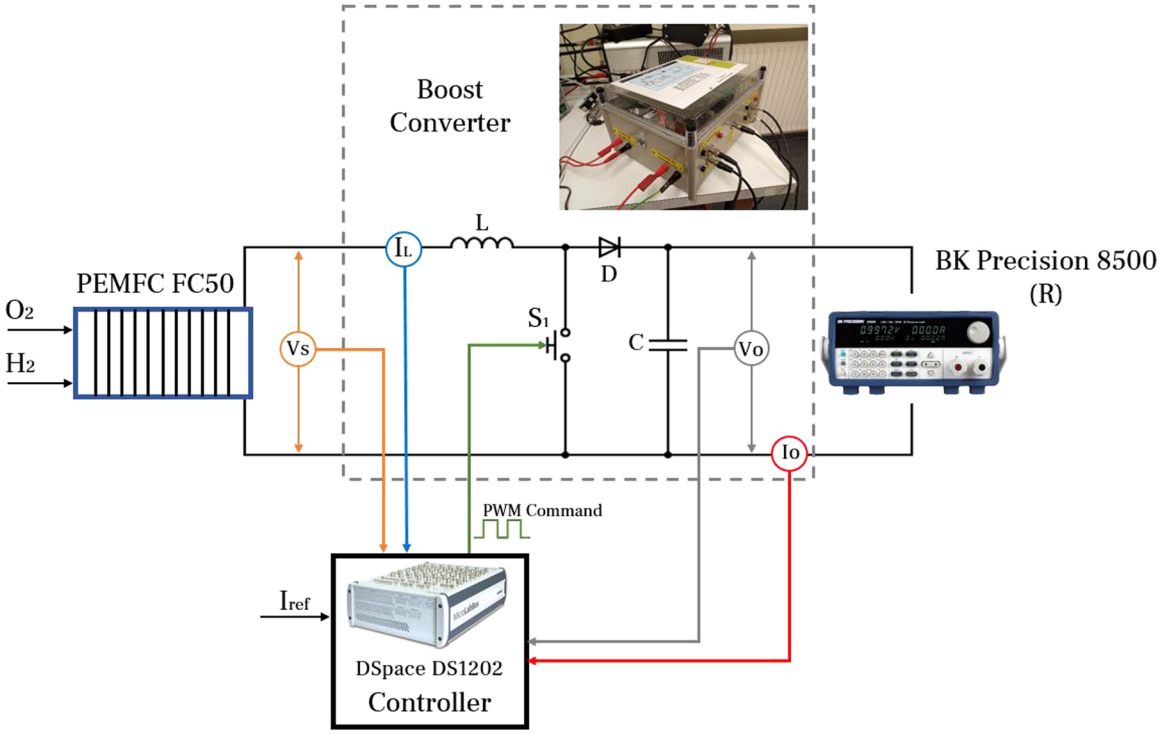

FIGURE 1 Hardware flow

generate C code in the hardware in an optimal way so that the designer can focus on the Simulink interface development. As previously mentioned, it also has the capacity to acquire which is mainly done by ControlDesk. The latter is a dSPACE software that records information in real-time and with further capabilities to provide parameters tuning that were previously configured in Simulink.

2.2 | Control designs

In this research, we aimed to design controllers which could follow a reference current named I_{ref} and established in Derbeli et al.[41] The involved structures are an FLC-T1 and FLC-T2 which will be explained in the following section. Major contrasts are in terms of robustness, control signal, and capacity for tracking. Therefore, we define the error in terms of the current to be followed as Equation (1); in this expression, I_L represents the measured output current of the fuel cell (which can be seen in Figure 1.

$$e = I_{ref} - I_L. \tag{1}$$

The duty cycle d is driven by the MicroLabBox through the PWM signal. Hence, it also has a straight relation to the output (V_o) and stack voltages (V_s). This implies that there are two diverse switching states that are best described by the system of Equation (2).

$$\begin{cases} \begin{bmatrix} \frac{di_L}{dt} \\ \frac{dV_{out}}{dt} \end{bmatrix} = \begin{bmatrix} 0 & \frac{-(1-d)}{L} \\ \frac{(1-d)}{C} & -\frac{1}{RC} \end{bmatrix} \cdot \begin{bmatrix} i_L \\ V_o \end{bmatrix} + \begin{bmatrix} \frac{1}{L} \\ 0 \end{bmatrix} V_s \\ y = [0 \quad 1] \cdot \begin{bmatrix} i_L \\ V_o \end{bmatrix} \end{cases} \tag{2}$$

The previously mentioned relation is mirrored in Equation (3), in which the duty cycle relates the stack and output voltage sources.[42] Applying Omh's law to the previously defined equation, an equivalent resistance where the duty cycle and the BK Precision 8500 come out in Equation (4). This is an equivalent resistance that changes with d. This relation allows changing the resistance perceived by the PEMFC so that for high values of the duty cycle, the equivalent resistance is lower.[43] It should be noted that the duty cycle must be between 0 and 1 which may represent a restriction for the control design.

$$V_{out} = \frac{V_s}{1-d}, \tag{3}$$

$$R_{eq} = (1-d)^2 R_{Out}. \tag{4}$$

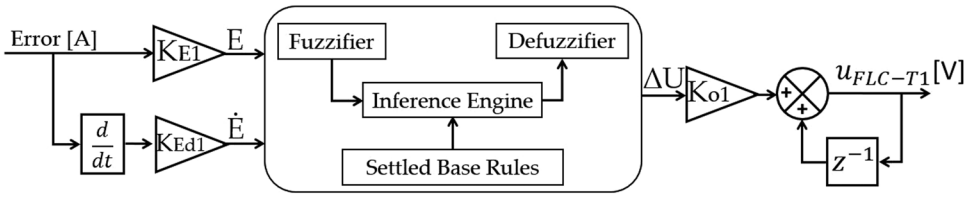

FIGURE 2 FLC-T1 control structure

The embedded controllers had parameters that we had to choose based on the desired performance. Because in this case, the goal is the reference tracking of the current, the error reduction was crucial. Hence, the minimization of the integral of the absolute error (IAE) is a tool that helps in tracking problems when variables need to be changed in real-time.[44–46] The expression is defined in Equation (5) where e_i is the error in the ith sampling, Δt is the sampling time and N is the number of samples chosen.[47]

$$\text{IAE} = \sum_{i=1}^{N} |e_i| \Delta t. \tag{5}$$

2.3 | Fuzzy logic type-1

The fuzzy logic principle is based on rules and constraints whose intention is to model the knowledge of an expert on a specific system.[48] The main structure is explained in Figure 2. FLC-T1 is characterized by three main steps, that are features of a Mamdami system[49,50]:

1. Fuzzification: the inputs (which in this case had been chosen as the normalized error and its derivative) are initially crisp values and need to be designated with fuzzy sets according to member functions.[51] Hence, type-1 sets are defined as a set A based on a universe X that belongs to a domain [0, 1], such that $A = \{(x, \mu_A(x)) | x \in X\}$ and μ_A range is between 0 and 1.[52] Latter mentioned is defined based on linguistic variables, which are words or sentences that correspond with the numerical values.[53]
2. Inference: is a rule-based method where the main logic from an expert is interpreted by *If–then* rules in linguistic mode.[54] The establishment of these rules is defined in Table 2 which relates the condition of the error and its derivative for consequent action. The values, that range between −1 and 1, are established and discretized as: negative big (NB, −1), negative medium (NM, −0.66), negative small (NS, −0.33), zero (Z, 0), positive small (PS, 0.33), positive medium (PM, 0.66) and positive big (PB, 1). The geometry and values of Table 2 were achieved after several tries from previous experiments.
3. Defuzzification: The process to get back to numerical values is performed in this step where the mechanics of (1) are inverted to return crisp values.[55,56] Previous rules are matched with discretized and uniform constants in the range of [−1 1] (Table 2).

TABLE 2 FLC linguistic rules

Ė / E	NB	NS	Z	PS	PB
NB	NB	NM	NM	NS	Z
NS	NM	NM	NS	Z	Z
Z	NM	NS	Z	PS	PM
PS	Z	Z	PS	PM	PM
PB	Z	PS	PM	PM	PB

Additional details of FLC-T1 are the gains K_{E1} and K_{Ed1} whose intention is to normalize the values of the error and its derivative. This is mainly because the fuzzifier process was developed with inputs of [−1, 1]. This is mainly because we configured the input membership functions within overlapped symmetric and triangular membership rules (shown in Figure 3). On the other hand, the gain K_{o1} aims to augment the output value of the fuzzy signal generation process. The mentioned gains were calibrated based on the minimization of the IAE as we formerly explained.

2.4 | Fuzzy logic type-2

Not only one of the disadvantages of FLC-T1 is the computational requirement when a behavioral description is complex (translated as the increment of *If–then* rules) but also when the expert knowledge is inappropriately defined. In this sense, FLC-T2 has been developed to consider uncertainties of the system dynamics.[57] The basic structure is provided in Figure 4. The main difference in contrast with FLC-T1 comes in the definition of the membership rules which have a defined uncertainty as an area instead of a

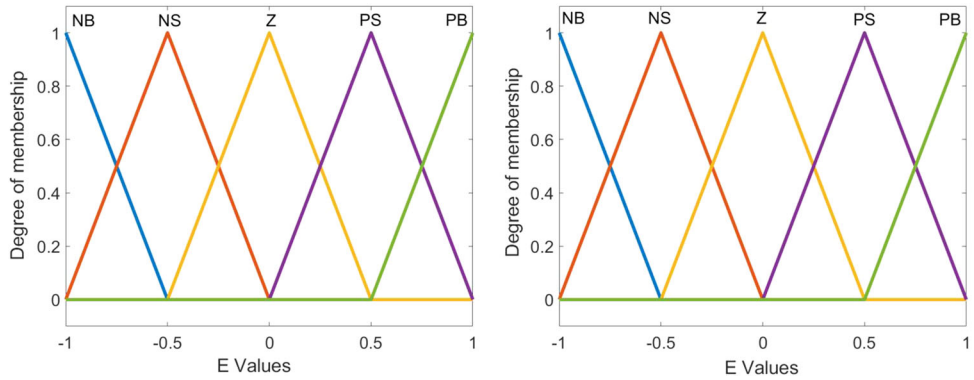

FIGURE 3 FLC-T1 membership functions

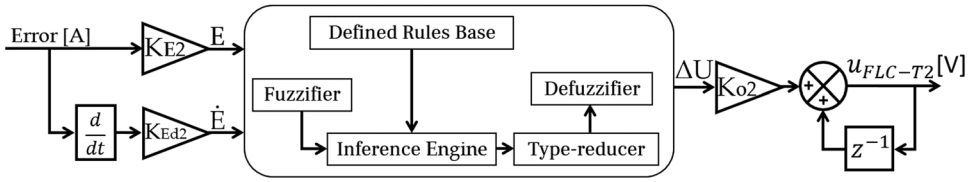

FIGURE 4 FLC-T2 control structure

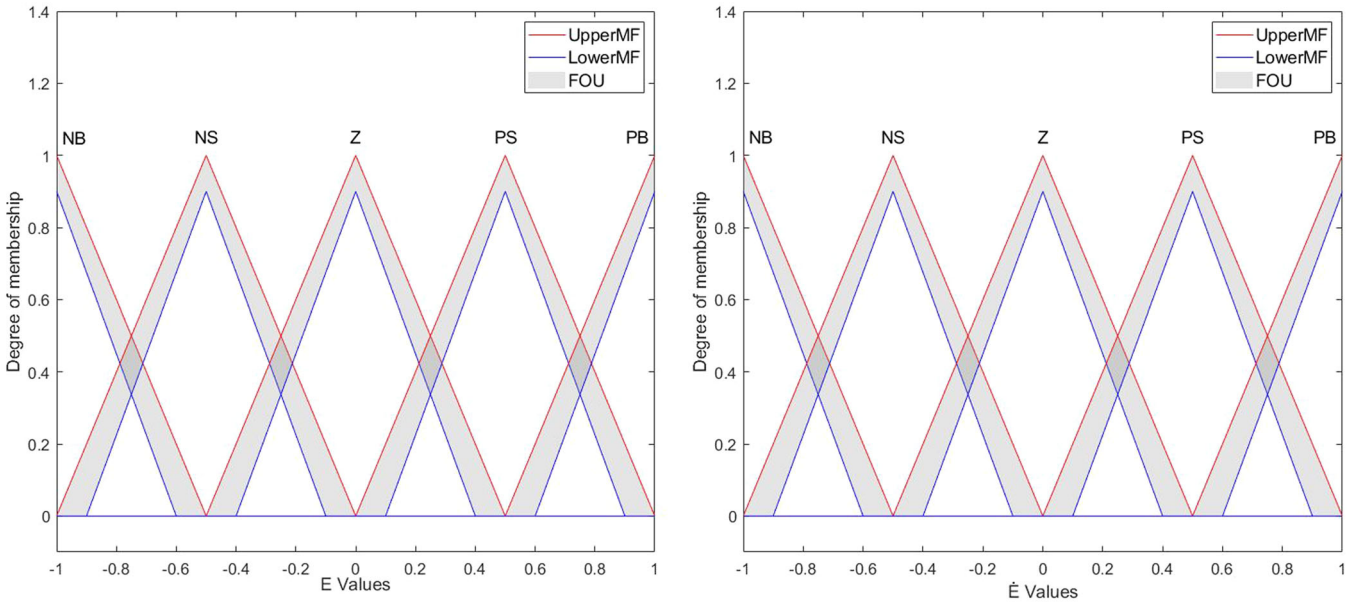

FIGURE 5 FLC-T2 membership functions

linear relation; this can be seen in a comparison between Figures 3 and 5.

The previous mentioned area is also known as the footprint of uncertainty (FOU) and it is limited between a lower and upper membership function for each case.[58,59] During the experiments that we carried out, we considered a 10% of uncertainty in respect to the membership functions defined for FLC-T1. This value has already been considered in former investigations where FLC-T2 was involved.[60]

The defuzzification has an extra process in this case, which is called "type-reducer." The name is mainly because the intention is to "reduce" from FLC-T2 to FLC-T1 by means of a center-of-gravity value calculation.[61] In this case, we used the "Karnik-Mendel" algorithm whose intention is to seek critical spots which could define the

centroid of an interval between both membership functions.[62] Also, this algorithm is commonly used in research for its efficiency.[63–65]

3 | EXPERIMENTAL RESULTS

The explained controllers were embedded in the dSPACE platform and the outcomes are described in this section. A step load whose value varied between 20 and 50 Ω, was increased at $t = 10.25$ s and decreased at $t = 30.2$ s. Hence, under these conditions and due to these perturbations, we were able to analyze dynamics and steady-state performance. In regard to the parameters obtained as a consequence of the minimization of the MSE, RMSE, and RRMSE, these are summarized in Table 3, where the parameters of the metrics are enlisted in Table 4. As it is noticeable from Table 3, we used the same parameters for the two fuzzy schemes proposed, aiming to point out the features of each controller. On the other hand, Table 4 proves the effectiveness of FLC-T2 over FLC-T1 since it reduces the MSE, RMSE, and RRMSE, respectively by 4.29%, 2.18%, and 2.18%.

First, our objective is to track a 4 A current on the PEMFC and the waveforms of the experiments performed are presented in Figure 6. Despite that, in this case, the controllers followed a similar path, and the improvements are noticed in a detailed numerical comparison based on Table 5, Figure 6B–D. In regard to robustness comparison, overshoots, undershoots, and response times (RT) were compared.

TABLE 3 Parameters achieved for the fuzzy logic type-1 and type-2 controllers

Parameters	
K_{E1}, K_{E2}	5
K_{Ed1}, K_{Ed2}	0.02
K_{o1}, K_{o2}	0.003

TABLE 4 Comparison of the different metrics

	MSE (A)		RMSE (A)		RRMSE (A)	
	Value	Difference	Value	Difference	Value	Difference
FLC-T1	0.0884	–	0.2974	–	7.4343	–
FLC-T2	0.0846	4.29%	0.2909	2.18%	7.2714	2.18%

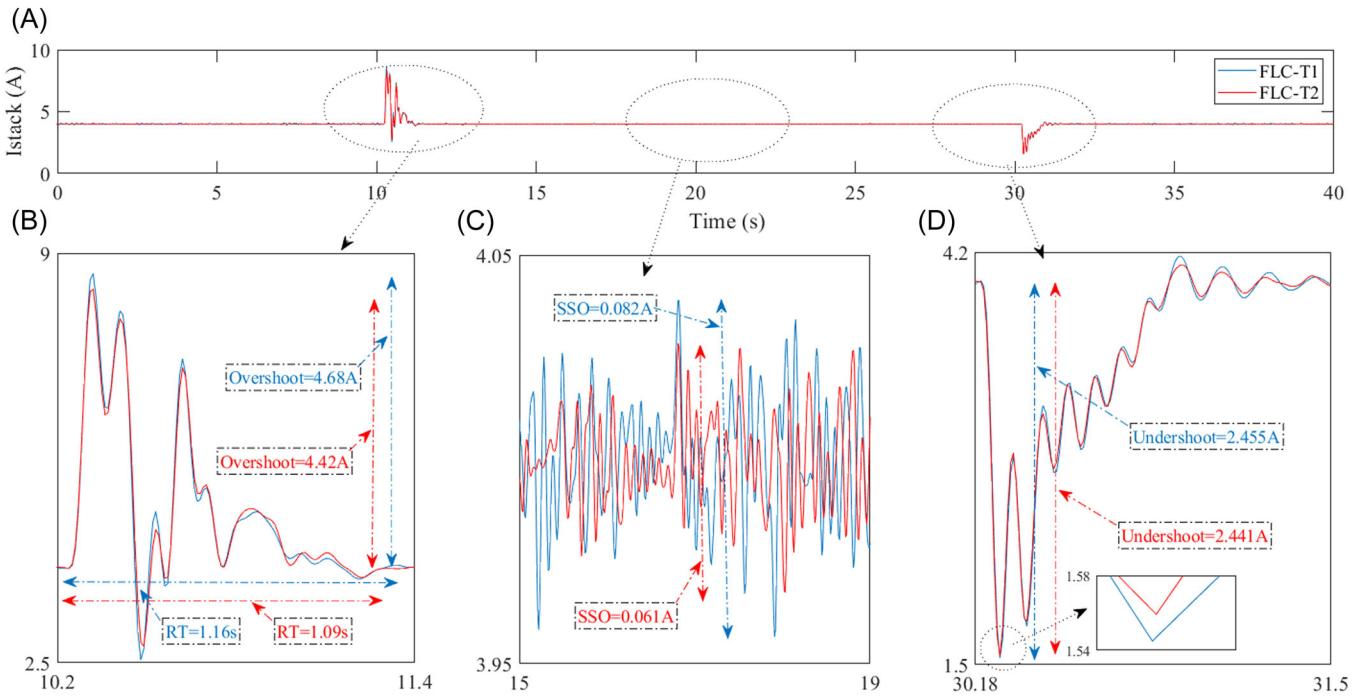

FIGURE 6 (A) Stack current signal, (B) influence of the first load variation, (C) steady-state oscillation, and (D) influence of the second load variation

TABLE 5 Comparison of the evaluated features

	Overshoot (A)		Undershoot (A)		SSO (A)		RT (s)	
	Value	Difference	Value	Difference	Value	Difference	Value	Difference
FLC-T1	4.68	–	2.455	–	0.082	–	1.16	–
FLC-T2	4.42	5.6%	2.441	0.57%	0.061	25%	1.09	6.03%

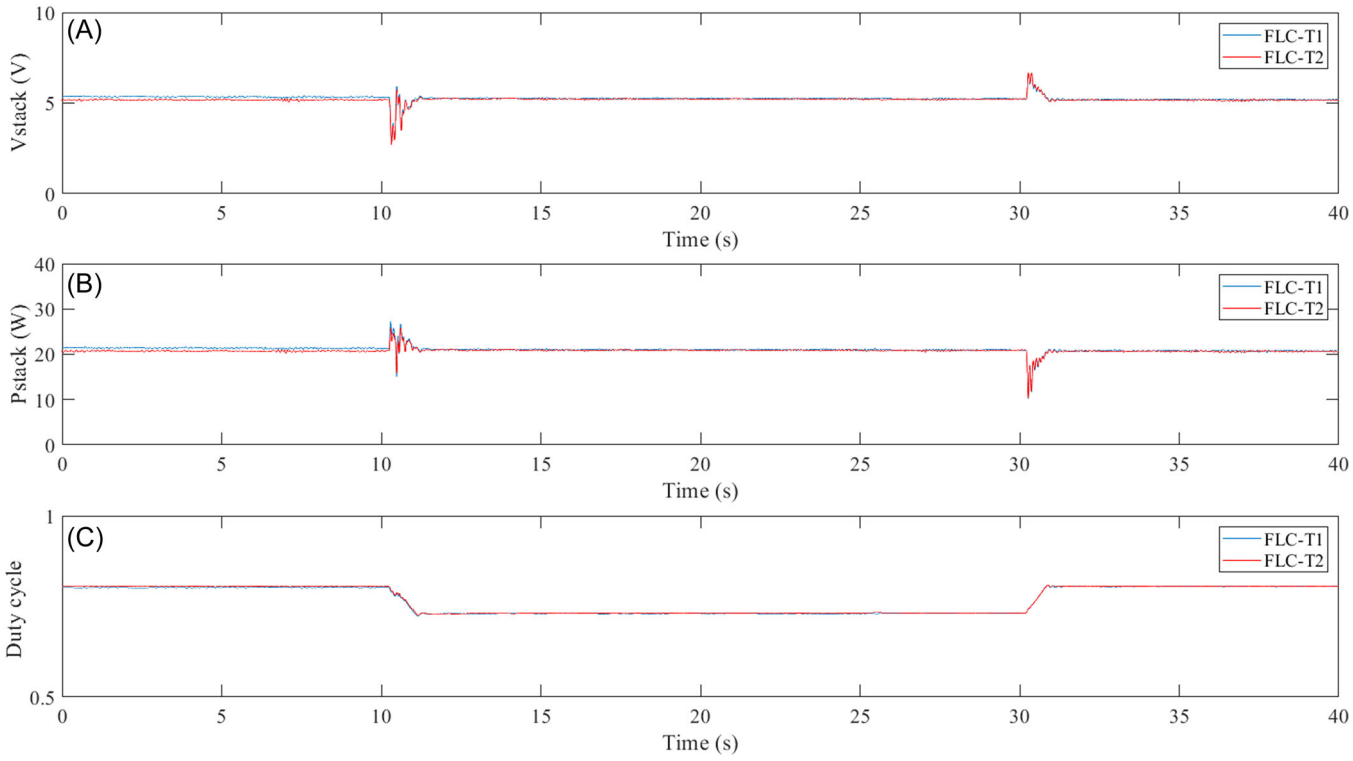

FIGURE 7 (A) Stack voltage signal, (B) stack power signal, and (C) duty cycle signal

As Figure 6B presents, the overshoots for the FLC-T1 and FLC-T2 were 4.68A and 4.42A, respectively. This means that FLC-T2 reduced this feature by 5.6% in contrast to FLC-T1. Also, individual RTs developed a significant enhancement: whereas FLC-T1 presented 1.16s, FLC-T2 trimmed this value to 1.09s. This implies that FLC-T2 still carried on with the best performance trend since the difference was around 6.03%. We can also analyze the undershoot demeanor when the resistance moved backward to the initial value at 30.2 s. In this sense, FLC-T1 developed an undershoot of 2.445A whereas FLC-T2 provided a reduction until 2.441A. Therefore, FLC-T2 had an enhancement of 0.57% in comparison to the alternative structure.

Response times had a higher difference to be appreciated and to evaluate the speed of each algorithm. These were achieved from Figure 6B by an estimation between the overshoot and its establishment. Hence, the FLC-T1 accomplished an RT of 1.16 s and FLC-T2 diminished the value at 1.09 s. This indicates a progress of 6.03% when the FLC-T2 was embedded.

On the other hand, steady-state oscillations (SSO) were checked as well. This is an important parameter because it shows the capabilities of the controllers when a constant reference needs to be followed when an external perturbation (like the resistance change) is executed and how's the variation along the time. In this case, the amplitude current amplitude was evaluated as in Figure 6B. Hence, FLC-T1 shows an average amplitude of 0.082 A, and FLC-T2 had a significant decrease of 0.061 A. Thus, FLC-T2 was able to improve a 25% in contrast to FLC-T1.

Figure 7 shows other important variables acquired during the experiment. The stack voltage and power are represented in Figures 7A,B. For the two control structures, power and voltage tend to have a constant performance of around 5 V and 20 W, respectively. Nevertheless, there are slight exceptions to the constants during the resistance switching as would be expected. Also, we inspect if relevant

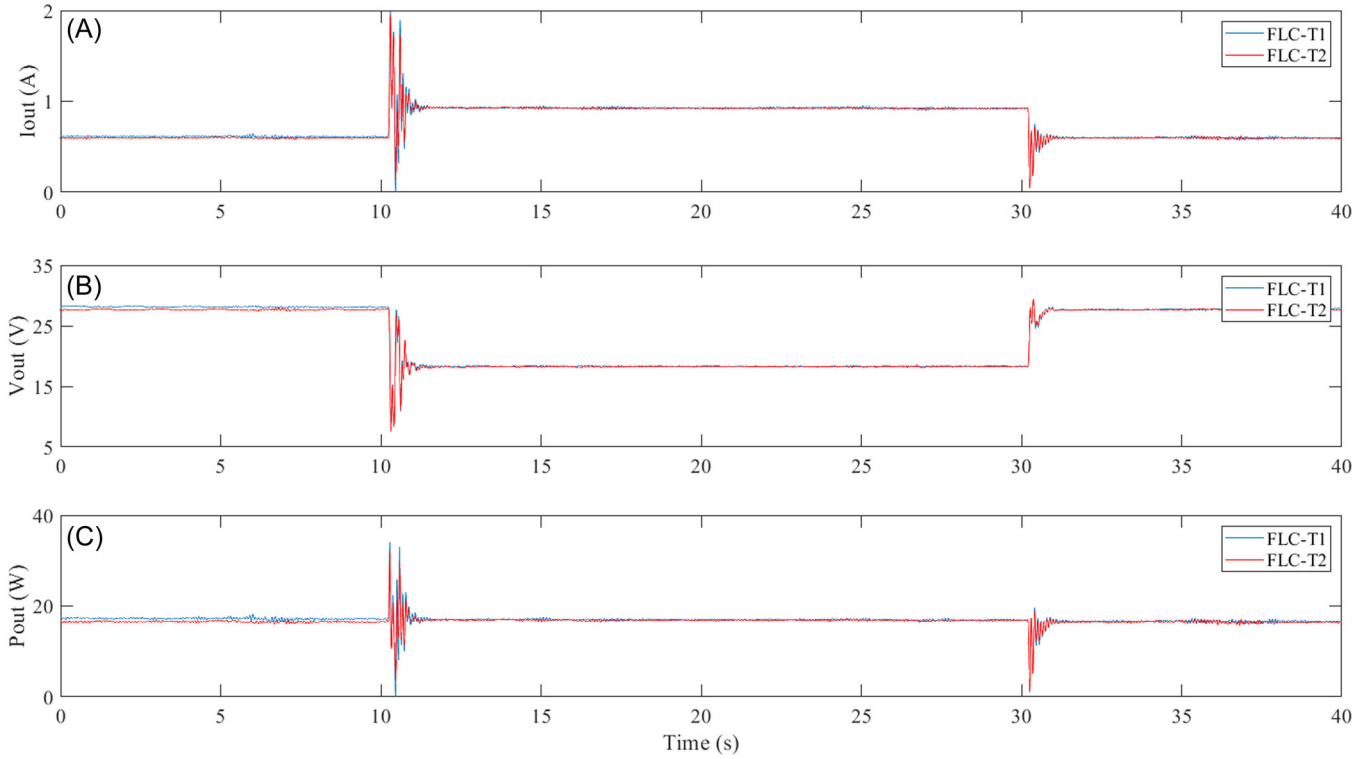

FIGURE 8 Boost converter output current, output voltage, and output power

values can cause spikes that may reach the PEMFC shutdown generated by the security system when the resistance was engaged. The evaluation of the formerly mentioned figures shows that the voltage or current of both controllers are in the range of the operating values which were previously detailed in Table 1. Another detail to be highlighted is a slight gap between the signals, which is noteworthy during the first 10.25 s. This phenomenon is produced since the experiments were carried out in different moments and because the environment temperature changed, it induced this difference. It is also important to take into account that slight amplitude differences (especially during the resistance changes) in the stack power and voltage are meaningful because the stack current was the variable to be followed. Figure 7C is the duty cycle generated as a control signal from the dSPACE platform. It is important to verify that its value is between 0 and 1 without substantial changes. It can be seen in this figure that the signal is between 0 and 1 whereas any vital shifts are detected for both FLCs.

Finally, boost converter output variables are shown in Figure 8. We recorded these to check if the control structures could generate any damage to the device. The output current of Figure 8A,B comprises values of current and voltage which are in the acceptable range of operation for both control structures when the external resistance changes. In regard to Figure 8C where the output boost converter power is detailed, it can be seen that in a steady state, the output power is around 18 W. This value differs from the one produced by the PEMFC due to the electrical losses that the boost converter components generate.

4 | CONCLUSIONS

In this article, we proposed a novel contrast of two fuzzy set configurations employed in a PEMFC system linked to a boost converter. The objective was to track a reference current that could be configured by a user. The control schemes that we used were fuzzy logic type sets defined as FLC-T1 and FLC-T2.

It has been shown that FLC-T1 is a control scheme defined through expert knowledge of a system based on membership functions and linguistic rules. On the other hand, FLC-T2 grants an extra degree with the inclusion of uncertainty when there are hesitations in the definition of the membership functions. This induces an extra complexity as it is needed an additional step for calculation known as “type-reducer.” Both of these structures had been designed and implemented in a real-time platform.

Our test rig platform was a commercial PEMFC manufactured by Heliocentris whose model is FC-50.

Since the voltage was low for an end-user role, we included a boost converter TEP-192 in the hardware configuration. Because the boost converter can be controlled with a PWM signal, the generator of this was through a dSPACE platform which also allowed the acquisition of data for the postprocessing. Additionally, a programmable load was added to the circuit to simulate an external load. The used reference was settled as 4 A with an external load change that began with a step-up at 10.25 s that lifted from 20 to 50 Ω and lowered back at 30.2 s.

Experimental outcomes showed the advantages that FLC-T2 could develop in the implementation. These were analyzed in-depth for the variable to be followed which was the stack current and we observed major differences in robustness and response time. FLC-T2 showed the best performance when the external resistance value climbed in terms of overshoot and response time. Also during the steady state and resistance fall, the FLC-T2 was still developing the most suitable demeanor in terms of oscillation and undershooting.

On the other hand, we also recorded the stack voltage and power. These showed a similar waveform in both controllers where any complex situations that could reach the PEMFC shutdown were seen. Also, the control signal named as duty cycle was investigated and any unpleasant behaviors were seen during its action. Finally, the boost converter output variables were also analyzed. They showed a good performance for the tested situations in which certain differences that were unrelated to the controllers' evaluation.

As future guidelines, the options can be related to different type-reducer algorithms for the FLC-T2. This can be a kick-off to calculate the computational time that each algorithm can require and thus, not only the control performance can be contrasted but also an improvement for hardware requirements can be presented. Additional paths related to the adaptation of parameters of each tested controller would increase the intelligence capability of the controllers. Also, in this research, both control algorithms were embedded for reference tracking but it would be an interesting proposal to use them for maximum power point tracking. This would highlight the performance of the fuzzy controllers from another perspective in terms of efficiency.

ACKNOWLEDGMENTS

The authors wish to express their gratitude to the Basque Government, through the project EKOHEGAZ (ELKARTEK KK-2021/00092), to the Diputación Foral de Álava (DFA), through the project CONAVANTER, and to the UPV/EHU, through the project GIU20/063, for supporting this work.

CONFLICT OF INTEREST

The authors declare no conflict of interest.

ORCID

Cristian Napole http://orcid.org/0000-0003-2639-9016
Mohamed Derbeli http://orcid.org/0000-0002-5804-7982

REFERENCES

1. Kong J, Oh S, Kang BO, Jung J. Development of an incentive model for renewable energy resources using forecasting accuracy in South Korea. *Energy Sci Eng*. 2021;10(9):3217-3688.
2. Napole C, Derbeli M, Barambones O. A global integral terminal sliding mode control based on a novel reaching law for a proton exchange membrane fuel cell system. *Appl Energy*. 2021;301:117473. https://www.sciencedirect.com/science/article/pii/S0306261921008606
3. Mahapatra MK, Singh P. Chapter 24—Fuel cells: energy conversion technology. In: Letcher TM, ed. *Future Energy*. 2nd ed. Elsevier;2014:511-547.
4. Zhao N, Zhang Y, Li B, et al. Natural gas and electricity: two perspective technologies of substituting coal-burning stoves for rural heating and cooking in Hebei Province of China. *Energy Sci Eng*. 2019;7(1):120-131.
5. Pagliaro M. Renewable energy in Russia: a critical perspective. *Energy Sci Eng*. 2021;9(7):950-957.
6. Cao Y, Li Y, Zhang G, Jermsittiparsert K, Nasseri M. An efficient terminal voltage control for PEMFC based on an improved version of whale optimization algorithm. *Energy Reports*. 2020;6:530-542.
7. Un-Noor F, Padmanaban S, Mihet-Popa L, Mollah MN, Hossain E. A comprehensive study of key electric vehicle (EV) components, technologies, challenges, impacts, and future direction of development. *Energies*. 2017;10(8):1217.
8. Lee SW, Do HL. High step-up coupled-inductor cascade boost DC-DC converter with lossless passive snubber. *IEEE Trans Industr Electron*. 2018;65(10):7753-7761.
9. Wang Y, Qiu Y, Bian Q, Guan Y, Xu D. A single switch quadratic boost high step up DC-DC converter. *IEEE Trans Industr Electron*. 2019;66(6):4387-4397.
10. Villegas Ceballos JP, Serna-Garcés SI, González Montoya D, Ramos-Paja CA, Bastidas-Rodríguez JD. Charger/discharger DC/DC converter with interleaved configuration for DC-bus regulation and battery protection. *Energy Sci Eng*. 2020;8(2):530-543.
11. Amirparast A, Gholizade-Narm H. Nested control loop design for differential boost inverter using generalized averaged model in photovoltaic applications. *Energy Sci Eng*. 2020;8(8):2734-2746.
12. Kodra K, Zhong N. Singularly perturbed modeling and LQR controller design for a fuel cell system. *Energies*. 2020;13(11):2375.
13. Woo CH, Benziger J. PEM fuel cell current regulation by fuel feed control. *Chem Eng Sci*. 2007;62(4):957-968.
14. Ghosh A, Banerjee S. A comparison between classical and advanced controllers for a boost converter. *2018 IEEE*

International Conference on Power Electronics, Drives and Energy Systems (PEDES); 2018:1-6.

15. Oates W, Smith R. Nonlinear optimal tracking control of a piezoelectric nanopositioning stage Proceedings of SPIE—The International Society for Optical Engineering; 2006:6166.
16. Napole C, Derbeli M, Barambones O. Fuzzy logic approach for maximum power point tracking implemented in a real time photovoltaic system. *Appl Sci*. 2021;11(13):5927.
17. Zhang S, Liu L, Cui X. Robust FOPID controller design for fractional-order delay systems using positive stability region analysis. *Int J Robust Nonlin Control*. 2019;29(15):5195-5212.
18. Mollaee H, Ghamari SM, Saadat SA, Wheeler P. A novel adaptive cascade controller design on a buck-boost DC-DC converter with a fractional-order PID voltage controller and a self-tuning regulator adaptive current controller. *IET Power Electron*. 2021;14(11):1920-1935.
19. Vu TNL, Chuong VL, Truong NTN, Jung JH. Analytical design of fractional-order PI controller for parallel cascade control systems. *Appl Sci*. 2022;12(4):2222.
20. Tepljakov A, Alagoz BB, Yeroglu C, Gonzalez E, HosseinNia SH, Petlenkov E. FOPID controllers and their industrial applications: A survey of recent Results. This study is based upon works from COST action CA15225, a network supported by COST (European Cooperation in Science and Technology). *IFAC—PapersOnLine*. 2018;51(4):25-30. 3rd IFAC Conference on Advances in Proportional-Integral-Derivative Control PID 2018.
21. Rakhtala SM. Self-tuning fuzzy logic PID controller with a practical view to PEM fuel cell air supply system. *Int J Modell Identification Control*. 2021;7(2):187-198.
22. Muñoz-Vázquez AJ, Fernández-Anaya G, Meléndez-Vázquez F, Sánchez Torres JD. Generalised conformable sliding mode control. *Math Methods Appl Sciences*. 2022;45(3):1687-1699.
23. Abbaker A. M. O, Wang H, Tian Y. Adaptive integral type-terminal sliding mode control for PEMFC air supply system using time delay estimation algorithm. *Asian J Control*. 2022;24(1):217-226.
24. Huangfu Y, Guo L, Ma R, Gao F. An advanced robust noise suppression control of bidirectional DC-DC converter for fuel cell electric vehicle. *IEEE Trans Transport Electrif*. 2019;5(4):1268-1278.
25. Yanarates C, Zhou Z. Fast-converging robust PR-P controller designed by using symmetrical pole placement method for current control of interleaved buck converter-based PV emulator. *Energy Sci Eng*. 2022;10(1):155-176.
26. Gutierrez SV, De León-Morales J, Plestan F, Salas-Peña O. A simplified version of adaptive super-twisting control. *Int J Robust Nonlin Control*. 2019;29(16):5704-5719.
27. Borlaug ILG, Pettersen KY, Gravdahl JT. The generalized super-twisting algorithm with adaptive gains. 2020 European Control Conference (ECC); 2020:1624-1631.
28. Marwa J, Dhahri S, Sellami A. Design of robust supertwisting algorithm based second-order sliding mode controller for nonlinear systems with both matched and unmatched uncertainty. *Complexity*. 2017;2017:1-8.
29. Rakhtala SM, Casavola A. Real-time voltage control based on a cascaded super twisting algorithm structure for DC-DC converters. *IEEE Trans Industr Electron* 2021;69(1):633-641.
30. Hernández-Vera B, Aguilar Lasserre AA, Gastón Cedillo-Campos M, Herrera-Franco LE, Ochoa-Robles J. Expert system based on fuzzy logic to define the production process in the coffee industry. *J Food Process Eng*. 2017;40(2):e12389.
31. 9—A PWA approach to Takagi-Sugeno fuzzy logic systems. In: Control and Estimation of Piecewise Affine Systems. Woodhead Publishing; 2014:169-192.
32. Tian Y, Chu Z, Ma G. Fuzzy logic control theory in clinical anesthesia. *Expert Syst*. 2022;39(3):e12761.
33. Yang B, Li J, Li Y, et al. A critical survey of proton exchange membrane fuel cell system control: summaries, advances, and perspectives. *Int J Hydrogen Energy*. 2022;47(17):9986-10020.
34. Samadi M, Rakhtala SM. Reducing cost and size in photovoltaic systems using three-level boost converter based on fuzzy logic controller. *Iran J Sci Technol Trans Electr Eng*. 2019;43(1):313-323.
35. Lu Y, Liu R, Wang K, Tang Y, Cao Y. A study on the fuzzy evaluation system of carbon dioxide flooding technology. *Energy Sci Eng*. 2021;9(2):239-255.
36. Shi J. A unified general type-2 fuzzy PID controller and its comparative with type-1 and interval type-2 fuzzy PID controller. *Asian J Control*. 2021;24(2):1808-1824.
37. Mosavi A, Qasem SN, Shokri M, Band SS, Mohammadzadeh A. Fractional-order fuzzy control approach for photovoltaic/battery systems under unknown dynamics, variable irradiation and temperature. *Electronics*. 2020;9(9): 1455.
38. Liu Z, Mohammadzadeh A, Turabieh H, Mafarja M, Band SS, Mosavi A. A new online learned interval type-3 fuzzy control system for solar energy management systems. *IEEE Access*. 2021;9:10498-10508.
39. Nabipour N, Qasem SN, Jermsittiparsert K. Type-3 fuzzy voltage management in PV/hydrogen fuel cell/battery hybrid systems. *Int J Hydrogen Energy*. 2020;45(56):32478-32492.
40. Kumar PS. PSK method for solving type-1 and type-3 fuzzy transportation problems. *Int J Fuzzy System Appl*. 2016;5(4):121-146.
41. Derbeli M, Napole C, Barambones O. Machine learning approach for modeling and control of a commercial heliocentris FC50 PEM fuel cell system. *Mathematics*. 2021;9(17):2068.
42. Derbeli M, Barambones O, Sbita L. A robust maximum power point tracking control method for a PEM fuel cell power system. *Appl Sci*. 2018;8(12):2449.
43. Omran A, Lucchesi A, Smith D, et al. Mathematical model of a proton-exchange membrane (PEM) fuel cell. *Int J Thermofluids*. 2021;11:100110.
44. Valdez F, Castillo O, Caraveo C, Peraza C. Comparative study of the conventional mathematical and fuzzy logic controllers for velocity regulation. *Axioms*. 2019;8(2):53.
45. Aole S, Elamvazuthi I, Waghmare L, et al. Active disturbance rejection control based sinusoidal trajectory tracking for an upper limb robotic rehabilitation exoskeleton. *Appl Sci*. 2022;12(3).
46. Napole C, Barambones O, Calvo I, Velasco J. Feedforward compensation analysis of piezoelectric actuators using artificial neural networks with conventional PID controller and single-neuron PID based on hebb learning rules. *Energies*. 2020;13(15):3929. https://www.mdpi.com/1996-1073/13/15/3929

47. Naranjo JE, Serradilla F, Nashashibi F. Speed control optimization for autonomous vehicles with metaheuristics. *Electronics*. 2020;9(4):551.
48. Rogulj K, Kilic Pamukovic J, Jajac N. Knowledge-based fuzzy expert system to the condition assessment of historic road bridges. *Appl Sci*. 2021;11(3):1021.
49. Espitia H, Soriano J, Machón I, López H. Design methodology for the implementation of fuzzy inference systems based on Boolean relations. *Electronics*. 2019;8(11):1243.
50. Islam SU, Zeb K, Din WU, et al. Design of robust fuzzy logic controller based on the Levenberg Marquardt algorithm and fault ride trough strategies for a grid-connected PV system. *Electronics*. 2019;8(4):429.
51. Tang X, Wang C, Hu Y, Liu Z, Li F. Adaptive fuzzy PID based on granular function for proton exchange membrane fuel cell oxygen excess ratio control. *Energies*. 2021;14(4):1140.
52. He W, Rodríguez RM, Dutta B, Martínez L. A type-1 OWA operator for extended comparative linguistic expressions with symbolic translation. *Fuzzy Sets Syst*. 2021;446:167-192.
53. Mendel JM. In: *Type-1 Fuzzy Sets and Fuzzy Logic*. Springer International Publishing; 2017:25-99.
54. Consiglio A, Casalino G, Castellano G, et al. Explaining ovarian cancer gene expression profiles with fuzzy rules and genetic algorithms. *Electronics*. 2021;10(4):375.
55. Chen S, Lin T, Jheng K, Wu C. Application of fuzzy theory and optimum computing to the obstacle avoidance control of unmanned underwater vehicles. *Appl Sci*. 2020;10(17):6105.
56. Fan Y, Mu A. Adaptive fuzzy proportion integration differentiation control in hydraulic offshore wind turbine for optimal power extraction based on the estimated wind speed. *Energy Sci Eng*. 2020;8(5):1604-1619.
57. Firouzi B, Alattas KA, Bakouri M, et al. A type-2 fuzzy controller for floating tension-leg platforms in wind turbines. *Energies*. 2022;15(5):1705.
58. Tabakov M, Chlopowiec A, Chlopowiec A, Dlubak A. Classification with fuzzification optimization combining fuzzy information systems and type-2 fuzzy inference. *Appl Sci*. 2021;11(8):3484.
59. Lin TC, Sun CW, Lin YC, Zirkohi MM. Intelligent contact force regulation of pantograph-catenary based on novel type-reduction technology. *Electronics*. 2022;11(1):132.
60. Indera-Putera SH, Mahfouf M, Mills GH. Blood-gas modelling for artificially ventilated patients using interval type-2 fuzzy logic system. XIV Mediterranean Conference on Medical and Biological Engineering and Computing 2016. Springer International Publishing; 2016:994-999.
61. Lee CL, Lin CJ. Integrated computer vision and type-2 fuzzy CMAC model for classifying pilling of knitted fabric. *Electronics*. 2018;7(12):367.
62. Chen C, Wu D, Garibaldi JM, John RI, Twycross J, Mendel JM. A comprehensive study of the efficiency of type-reduction algorithms. *IEEE Trans Fuzzy Syst*. 2021;29(6):1556-1566.
63. Ontiveros-Robles E, Melin P, Castillo O. New methodology to approximate type-reduction based on a continuous root-finding karnik mendel algorithm. *Algorithms*. 2017;10(3):77.
64. Tai K, El-Sayed AR, Biglarbegian M, Gonzalez CI, Castillo O, Mahmud S. Review of recent type-2 fuzzy controller applications. *Algorithms*. 2016;9(2):39.
65. Han S, Liu X. Global convergence of Karnik-Mendel algorithms. *Fuzzy Sets Syst*. 2016;283:108-119.

How to cite this article: Napole C, Derbeli M, Barambones O. Experimental validation of fuzzy type-2 against type-1 scheme applied in DC/DC converter integrated to a PEM fuel cell system. *Energy Sci Eng*. 2023;11:699-710.
doi:10.1002/ese3.1355